Eurographics Workshop on Visual Computing for Biomedicine (2008)
C. P. Botha, G. Kindlmann, W. J. Niessen, and B. Preim (Editors)

Automatic Hepatocyte Quantification from Histological Images: Comparing Pre-smoothing Filters

T. Ivanovska[1], A. Schenk[2], U. Dahmen[3], H. K. Hahn[1,2], L. Linsen[1]

[1] Jacobs University, Bremen, Germany
[2] MeVis Research, Bremen, Germany
[3] Department of General, Visceral and Transplantation Surgery, University Hospital Essen, Germany.

Abstract

Quantity of hepatocytes in the liver can reveal a lot of information for medical researchers. In our project, it is needed for evaluation of the liver regeneration rate. In this paper, we present a processing pipeline for automatic counting of hepatocytes from images of histological sections. In particular, we propose to introduce a preprocessing step in form of image smoothing. We apply five different smoothing techniques, namely Gaussian smoothing, nonlinear Gaussian smoothing, median filtering, anisotropic diffusion, and minimum description length segmentation, and compare them to each other. The processing pipeline is completed by subsequent automatic thresholding using Otsu's method and hepatocyte detection using Hough transform. We compare the quantification results in terms of quality (sensitivity and specificity rates) against the manually specified ground truth. We discuss the results and limitations of the individual processing steps as well as of the overall automatic quantification approach.

Categories and Subject Descriptors (according to ACM CCS): I.4.6 [Image Processing and Computer Vision]: Segmentation

1. Introduction

Quantification of defined cell types in histology is frequently needed. One example where quantification of a defined cell type is necessary is the determination of the hepatocyte proliferation index. The liver has the unique ability to regenerate in response to injury or loss of liver mass. One well accepted way to describe the kinetics of this process is to quantify the relative proportion of dividing hepatocytes, the functional parenchymal cells in the liver, at different time points after the liver injury.

Dividing hepatocytes can be identified by special immunohistochemical staining techniques of the hepatocyte nuclei such as the BrdU-Staining. A sample of the liver, about 0.5-1cm^3 in size, has to be formalinfixed and paraffinembedded. After cutting sections of about $4-6\mu m$ thickness they are subjected to a special immunohistochemical staining procedure. Nuclei of dividing cells, hepatocytes, but also other non-parenchymal stromal cells, are marked in one color, e.g. red, whereas the nuclei of the non-dividing cells are marked with a counterstain, e.g. blue. The proliferation index can be calculated after determining the number of proliferating hepatocytes with a red nucleus and the total number of hepatocytes with either a red or a blue nucleus.

In the past, the proliferation index was determined by simple counting of proliferating and non-proliferating cells using a sample size of 1000 to 3000 hepatocytes. This is a time-consuming procedure requiring an experienced observer, who is trained to discriminate hepatocytes from the other cells types in the liver. With the availability of digital photography, the counting process can be done on the image by marking the target cell using a simple image analysis performed with such software as Image Tool (see http://ddsdx.uthscsa.edu/itdesc.html/). The results of the counting procedure can be documented by saving the overlay image with the marked target cells.

It is very appealing to develop an algorithm for automated quantification of defined target cells in histology as the quantification process should be less labor-intensive. When developing an algorithm for quantification of a defined target cell type, the key challenge is to achieve a highly reproducible and unequivocal differentiation between the target cell and other cells. Furthermore, a number of difficul-

ties with respect to the image quality have to be overcome. Images of stained sections are subject to variations in the color properties (e.g., intensity or saturation) due to small differences in the histological processing of the tissue sample, which consists of several non-automatic steps. Variations may include thickness of the section and contact time of the section with the different staining solution, but may also occur during image acquisition (camera settings).

The goal of this study is to obtain a fully automated method for quantifying the number of hepatocytes on histological images of rat livers. We propose an image processing pipeline that is based on image smoothing as a preprocessing step. We discuss different smoothing techniques for image preprocessing and compare the overall results to the images obtained by manual hepatocyte counting, which are considered as the ground truth.

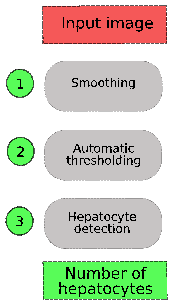

Figure 1: Flowchart for automatic hepatocyte quantification.

In Figure 1, the overall processing pipeline of our algorithm is depicted. The initial images appear to be quite noisy and hinder a satisfying direct hepatocyte detection. We propose to process images first in such a way that the amount of all other structures besides the hepatocytes is reduced, while the resulting image still contains all important information about them. For the applied staining of the hepatocytes, it can be observed that all of them are visible in the red color channel, while the proliferating hepatocytes are easily distinguishable in the blue color channel. We apply the smoothing filters to the corresponding channels of the image. Furthermore, we compare five methods for the image smoothing which described in detail in Section 3.

The second part of our algorithm consists of a sequence of processing steps that are applied to the smoothed images. We automatically distinguish between the hepatocytes and background by utilizing Otsu thresholding, see Section 4. In order to estimate the number of different hepatocytes in an image, we still need to take care of non-hepatocyte regions with similar colors and regions with overlapping hepatocytes. These problems are dealt with using an edge detection followed by a Hough transform, see Section 4.

As a result, we obtain circles that depict the position and size of the detected hepatocytes. In Section 5, we show the intermediate and final results of our processing pipeline and compare the results obtained by different preprocessing methods.

2. Related Work

Although a lot of automatic image processing approaches for histological sections have been developed, it is difficult to compare them to each other due to the difference of the staining methods applied to the data and the related image analysis problems. Most of the methods in this area are aiming at a precise boundary detection. For example, methods for nuclei segmentation using basic fuzzy c-means clustering [LSP03] or adaptive thresholding [PGH*06] have been proposed. These methods seem to have difficulties when dealing with images showing large variability in the histology staining.

A more sophisticated approach based on active contour models [BL98] seems to be less sensitive to staining variability and produces decent results as long as the nuclei are non-overlapping. Overlapping nuclei are not handled appropriately.

Naik et al. [NDA*08] proposed to integrate several levels of image information to segment gland and nuclei in breast and prostate cancer images. For nuclei segmentation the template matching scheme has been used. The templates have been selected according to the size and the elliptical shape of the nuclei, which correlates in some sense to the last step of our processing pipeline.

Datar et al. [DPC08] proposed to use hierarchical self-organizing maps to segment four types of tissue, namely glands, epithelia, stroma, and nuclei, but it is not suitable for separating the individual cells in order to determine their quantity.

3. Smoothing Methods

According to the flowchart depicted in Figure 1, the first processing step is to smooth the histological images. We have chosen to apply and compare the following techniques for this preprocessing step: Gaussian smoothing, non-linear Gaussian smoothing, median filtering, anisotropic diffusion, and minimum description length (MDL) segmentation. The MDL approach [Ris87] allows for simultaneous denoising and segmentation. Our choice has been motivated by the following considerations. The Gaussian filtering technique is a simple standard approach to image denoising. Median, anisotropic diffusion, and non-linear Gaussian filters are non-linear, denoising, and edge-preserving approaches. In addition, we decided to use an MDL segmentation technique with a piecewise constant image model to check, whether a local spatial segmentation algorithm can give some advantages in this task. In the following, we describe all methods in more detail.

3.1. Gaussian Smoothing

The Gaussian smoothing operator is a 2D convolution operator. It removes detail and noise and thus blurs images. The idea of Gaussian smoothing is to use this 2D distribution as a "point-spread" function, which is achieved by convolution. It uses a kernel that represents the shape of a Gaussian ("bell-shaped") hump. A 2D Gaussian has the form:

$$G(x,y) = \frac{1}{2\pi\sigma^2} \exp\left(-\frac{x^2+y^2}{2\sigma^2}\right), \tag{1}$$

where (x,y) are spatial positions and σ^2 is the (constant) noise variance.

3.2. Nonlinear Gaussian Smoothing

This method uses simple non-linear modifications of Gaussian filters [AMG98]. In the literature it is also referred as bilateral filter. There are several independently discovered variations and extensions [TM98, PD06, DD02]. Let I be a signal function and $g_{\sigma_x}(t) = \exp\left(\frac{-t^2}{2\sigma_x^2}\right)$ a Gaussian function, then their convolution product for a pixel p is defined as follows:

$$\begin{aligned} G_{\sigma_x} I(p) &= \frac{1}{N_{qp}} \sum_{q \in N_p} g_{\sigma_x}(\| q-p \|) I(q) \\ &= I(p) + \frac{1}{N_{qp}} \sum_{q \in N_p} g_{\sigma_x}(\| q-p \|)\,(I(q)-I(p))\,, \end{aligned} \tag{2}$$

where N_p is the neighborhood of pixel p and $N_{qp} = \sum_{q \in N_p} g_{\sigma_x}(\| q-p \|)$.

In order to preserve edges, a weight depending on the distance in color space between pixels p and its neighbor q is added to the convolution leading to the following expression:

$$\begin{aligned} &G_{\sigma_x,\sigma_z} I(p) \\ &= \frac{1}{N_{qp}} \sum_{q \in N_p} g_{\sigma_x}(\| q-p \|) g_{\sigma_z}(I(q)-I(p)) I(q). \end{aligned} \tag{3}$$

Aurich et al. suggest to use a sequence of three or five filters to achieve best results and give hints on how to choose appropriate values for σ_x and σ_z [AMG98].

3.3. Median Filter

The idea of median filtering is to examine a sample of the input and to decide whether it is a good representative for the signal. To do so, a window consisting of an odd number of samples is used, whose center lies at the currently examined pixel. For each pixel in the image, the values in the window are sorted numerically and the median value, i.e., the value of the sample located in the center of the window after sorting, is selected as the output.

3.4. Anisotropic Diffusion

Anisotropic diffusion filter is a non-linear smoothing filter that encourages intraregion smoothing while inhibiting interregion smoothing. It was initially formulated by Perona and Malik [PM90]. The continuous form for anisotropic diffusion is given by

$$\frac{\partial I}{\partial t} = div\,(g\,(\|\nabla I\|) \cdot \nabla I)\,, \tag{4}$$

where I denotes the image and function g is defined by

$$g\,(\|\nabla I\|) = \exp\left(-\left(\frac{\|\nabla I\|}{K}\right)^2\right)$$

with flow constant K. The discrete version of Equation (4) is given by

$$I_i^{t+1} - I_i^t + \lambda \sum_{j \in N_i} \left[(I_i^t - I_j^t) \exp\left(-\left(\frac{(I_i^t - I_j^t)}{K}\right)^2\right)\right] = 0,$$

where λ is a normalization factor. The discrete version is used to iteratively compute the image values I_i^{t+1} at iteration step $t+1$ from the image I_i^t at iteration step t, where I_i^0 describes the original image values.

3.5. MDL Segmentation

The fundamental idea behind the Minimum Description Length (MDL) principle is that any regularity in a given data can be used to compress the data [Ris87]. The image segmentation or image partitioning problem with respect to the MDL principle can be formulated as follows: Using a specified descriptive language, construct the description of an image that is simplest in the sense of being shortest [Lec89]. Let $L(M_i)$ denote the language for describing a model M_i and $L(D|M_i)$ the language for describing data D given model M_i. Moreover, let $|.|$ denote the number of bits in the description. The goal is to find the model M_i that minimizes the code length

$$C_l = |L(M_i)| + |L(D|M_i)|\,.$$

In terms of image segmentation the code length can be written as

$$C_l = |L(u)| + |L(I-u)|\,, \tag{5}$$

where the model we are looking for is the underlying image representation (or segmentation) u that minimizes the code length. The term I describes the initial (or given) image, and the difference $(I-u)$ between the given image I and the segmentation u corresponds to the noise in the image. The noise describes the data with respect to model u.

A simple implementation of the MDL principle for image segmentation was proposed by Leclerc [Lec89]. He assumed a piecewise constant image and derived the functional (or

energy term)

$$C_l = \frac{b}{2} \sum_{i \in Im} \sum_{j \in N_i} \left(1 - \delta\left(u_i - u_j\right)\right) + a \sum_{i \in Im} \left(\frac{I_i - u_i}{\sigma}\right)^2, \quad (6)$$

where u denotes the underlying image, I the given image, and σ^2 the noise variance. Moreover, $\delta(x)$ denotes the Kronecker delta, Im denotes the range of the image, and N_i is the neighborhood of the ith pixel. Coefficients a and b are constants. The formulated functional C_l is minimized, and the resulting underlying image is taken as the output.

4. Hepatocyte Detection

Taking the smoothed one-channel images as input, we separate the hepatocytes from the background using Otsu thresholding [Ots79]. Otsu thresholding assumes that the image exists of two classes (foreground and background) and operates on the histogram to find the optimal threshold to separate the two classes such that the within-class variance of the resulting classes is minimal. The within-class variance is computed as the weighted sum of the variances of each class:

$$\sigma^2_{within}(k) = P_1(k)\sigma_1^2(k) + P_2(k)\sigma_2^2(k), \quad (7)$$

where k is the threshold and P_i and σ_i^2 are the probability and the variance of class i, respectively. The output of this step can be stored in a binary image.

Next, we want to detect the hepatocytes, which appear in the images in form of round objects of an approximately known size. To achieve this, we use a Hough transform [Hou59] for circles detection in images. The goal of a Hough transform is to find (possibly imperfect) instances of objects within a certain class of shapes (circles in our case). It uses a voting procedure that is deployed in parameter space, where the desired shapes are identified as local maxima. The parametric equation of the circle is given by

$$(x,y) = (x_0,y_0) + r(\cos\theta, \sin\theta).$$

If the radius r of the circles is known, we need to find the center coordinates (x_0,y_0). An accumulator matrix is used to store the votes. Initially, it is filled with zeros. Then, for each non-black pixel (x,y) in the input image, the pair (x_0,y_0) is calculated and $acc[x_0,y_0]$ is increased by one. The local maxima in the resulting accumulator matrix correspond to the centers of the circular structures in the input image. The accumulator matrix is smoothed for more adequate result. To make the search for the circular structures simpler and faster, we first extract the boundaries from the binary images obtained by Otsu thresholding using simple Sobel operator and use the resulting image as input for the Hough transform algorithm.

Our implementation of the Hough transform is based on the one from the National Library of Medicine Insight Segmentation and Registration Toolkit (ITK) (see http://www.itk.org/). However, we modified it to avoid the fixed number of circles as a user-defined parameter. Instead, the search for circles stops when the height of the currently detected maximum in the accumulator array is smaller than a certain percentage of the first detected maximum. Each detected circle is checked against the binary image, and those circles that lie outside the regions are completely neglected.

Having detected the hepatocytes in form of circles given by the Hough transform, we can count the circles and the resulting number is the output of our automatic quantification algorithm. All the above-mentioned algorithms have been implemented, using MeVisLab, Software for Medical Image Processing and Visualization (see http://www.mevislab.de).

5. Results

To discuss the results we obtain using our approach with the different smoothing methods, we focus on the counting of the whole number of hepatocytes, which appears to be a challenging quantification task, as the hepatocytes stained with blue are often very hard to visually distinguish from the background.

We have made a series of tests on images from four different datasets and estimated the rates of true and false positives with respect to the ground truth information given in form of manually specified hepatocytes. The images are RGB images of size 2576×1932 with 8 bit color depth per channel. An example image is given in Figure 7. For the tests with different smoothing techniques we always chose exactly the same parameters for all the other steps of our pipeline. We took the following parameters for the smoothing filters. For Gaussian smoothing $\sigma = 4$; for Median filtering the kernel is 14×14; for Perona-Malik anisotropic diffusion the time step size is taken 7.4, the number of steps is 4, the edge parameter of the diffusivity function is 3.8, in each diffusion step the image is processed with Gaussian smoothing with parameter, equal 1.54; for bilateral filtering start values for σ_x and σ_z are 10 and 100 respectively and the chain of several filtering steps is used, where σ_x is increased and σ_z is decreased. In addition, we compared our results to the results that can be obtained without preprocessing. In the case of no pre-smoothing of the images, we observed that automatic thresholding using Otsu method does not work. We had to replace it with manual thresholding for each image. Thus, it was not possible to keep the entire pipeline fully automated. In fact, it turned out that the selection of the manual threshold was rather cumbersome, as we needed to tune the threshold for each image individually and the tuning was not as intuitive as expected.

For the MDL segmentation algorithm we had to cut regions of 1024×1024 out of the full-sized images and to evaluate the true and false positive rates on the smaller images, since the MDL-based method was implemented on the

GPU which was limited for a NVidia Quadro FX 4500 video card to this image size.

The results of our evaluation are presented in Table 1. The following notations for the headings are used: "Detected" means the number of circles found by Hough transform; "TP" is the number of True Positive hepatocytes, which is the result of the overlay of detected circles and the user expectations; "FN" denotes the number of False Negative hepatocytes, which is the difference between the Ground Truth Positives and the True Positives; "FP" stands for the number of False Positive hepatocytes, which is the difference between "Detected" and "TP"; "TN" is the number of True Negative hepatocytes, which is calculated as the difference between FP and the number of Ground Truth Negatives; and Ground P and Ground N are the number of Positive and Negative hepatocytes manually specified by the expert. The most important numbers are the computed sensitivities and specificities. Sensitivity is defined by $TP/(TP+FN)$ and measures the proportion of actual positives, while specificity is defined by $TN/(TN+FP)$ and measures the proportion of true negatives.

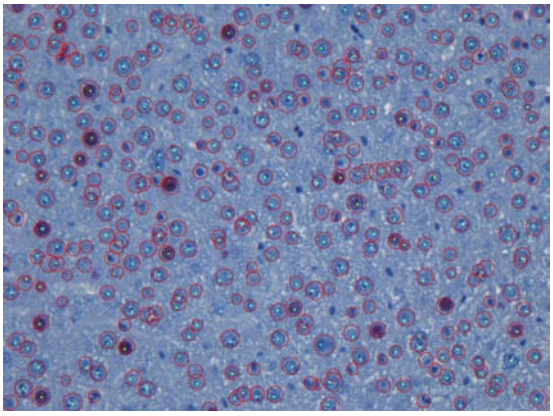

Figure 2: Overlay image for AEE-17-1 processed with anisotropic diffusion. A huge number of false positives occur. False positives are the detected circles without the corresponding green ground truth mark.

In Figure 5, several examples of our results and the manually defined ground truth images are depicted in an overlaid fashion. The hepatocytes marked with green dots represent the ground truth, while the red circles are the output of the Hough transform after applying our entire processing pipeline. The results for MDL segmentation methods are presented in Figure 3b. The images visually document the findings in Table 1.

6. Discussion and Future Work

As can be observed from Table 1, appropriate smoothing as a preprocessing step allows for reasonable quantification results. In general, anisotropic diffusion and non-linear Gaussian smoothing appear to be the most suitable methods for the given type of data. The MDL-based approach allows to smooth the image and reduce the number of colors (see Figure 3a) while preserving the important details, which is necessary to achieve a good segmentation. However, for the given quantification task, the MDL method does not give better results, as the overall goal is just the number of hepatocytes and not their perfect boundaries. Hence, the computational costs for the minimization procedure in MDL segmentation is not justified for our purposes.

Partially overlapping hepatocytes are no major problem of our approach, as Hough transform detects them correctly in most cases, see Figure 6b. However, when applying the described Hough transform we observed that some false hepatocytes are detected that cover only a small area of a circle, see Figure 6b. These small dark structures are Kupffer cells, another type of the cells in the liver, that should not be counted. We need to estimate the area of the overlapping circles and cells in the binary image and discard those with small area. This extension of the Hough transform step is a part of our future work.

We also observe from Table 1 that for image AEE-17-1 the specificity is extremely low and the number of false positives is correspondingly high, especially when using anisotropic diffusion or Gaussian smoothing. The results for anisotropic diffusion are presented in Figure 2. The problem is caused by the fact that there exist two different appearances of hepatocytes in the histological images of our study (see Figure 6a). The first type has the appearance of an approximately homogeneous region with blurred or crisp boundaries. These hepatocytes have a color that is darker than the background and they can be successfully detected with our approach. Such cells occur in most of the data sets. The second type has an appearance with crisp boundaries, but their interior has about the same color as the background. In Figure 6a the hepatocytes of the first type are marked with green and the ones of the second type are marked with red. For hepatocytes of the second type another processing step would need to be inserted into the processing pipeline, which is also a part of the future work.

Another challenge for our future work are images where portal or central veins are present, see Figure 4. In such a case the image cannot be processed successfully with Otsu thresholding, as now there are three main classes in the image: cells, background and the vein structure.

7. Conclusion

We have presented an automatic approach to hepatocyte quantification from histological images. The proposed processing pipeline consists of a smoothing step, an automatic thresholding using Otsu method, and a Hough transform. We tested different smoothing methods and discussed the

Total hepatocytes									
Image	Smoothing	Detected	TP	FN	FP	TN	Sensitivity	Specificity	Ground P/N
AEE-15-1	None	224	211	32	13	150	0.87	0.92	243 / 163
AEE-15-1	Gaussian	237	220	23	17	146	0.91	0.9	243 / 163
AEE-15-1	Nonlinear Gaussian	234	222	21	12	151	0.91	0.93	243 / 163
AEE-15-1	Median	227	219	24	8	155	0.9	0.95	243 / 163
AEE-15-1	Anisotropic Diff.	242	224	19	18	145	0.92	0.89	243 / 163
AEE-15-1^{region}	MDL	55	49	5	6	21	0.91	0.78	54 / 27
AEE-16-1	None	218	193	22	25	133	0.9	0.84	215 / 158
AEE-16-1	Gaussian	236	202	13	34	124	0.94	0.78	215 / 158
AEE-16-1	Nonlinear Gaussian	221	197	18	24	134	0.92	0.85	215 / 158
AEE-16-1	Median	199	184	31	15	143	0.86	0.91	215 / 158
AEE-16-1	Anisotropic Diff.	228	199	16	29	129	0.93	0.82	215 / 158
AEE-16-1^{region}	MDL	43	36	5	7	29	0.88	0.81	41 / 36
AEE-17-1	None	191	149	91	42	82	0.62	0.66	240 / 124
AEE-17-1	Gaussian	329	212	28	117	7	0.88	0.06	240 / 124
AEE-17-1	Nonlinear Gaussian	238	194	46	44	80	0.81	0.65	240 / 124
AEE-17-1	Median	307	211	29	96	28	0.88	0.23	240 / 124
AEE-17-1	Anisotropic Diff.	339	225	15	114	10	0.94	0.08	240 / 124
AEE-17-1^{region}	MDL	57	48	7	9	21	0.87	0.7	55 / 30
AEE-18-1	None	225	198	47	27	116	0.81	0.81	245 / 143
AEE-18-1	Gaussian	244	211	34	33	110	0.86	0.77	245 / 143
AEE-18-1	Nonlinear Gaussian	252	222	23	30	113	0.91	0.79	245 / 143
AEE-18-1	Median	246	219	26	27	116	0.89	0.81	245 / 143
AEE-18-1	Anisotropic Diff.	258	222	23	36	107	0.91	0.75	245 / 143
AEE-18-1^{region}	MDL	49	44	8	5	21	0.85	0.81	52 / 26

Table 1: Hepatocyte quantification results for four different data sets.

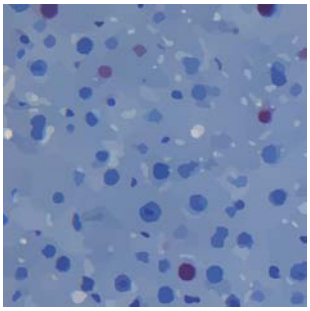

(a) Result of MDL-based segmentation algorithm (before applying automatic thresholding and Hough transform). The cell boundaries are well-preserved.

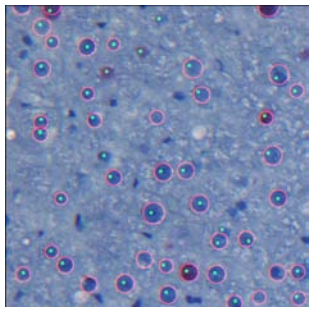

(b) Overlaying the output of Hough transform (red circles) with the manually specified output (green dots).

Figure 3: A region from image AEE-16-1 with MDL-based preprocessing step.

quantification results. Nonlinear Gaussian smoothing and anisotropic diffusion turned out to be the most suitable ones. In general, we achieved reasonable quantification results in terms of specificity and sensitivity. The pre-smoothing step was necessary in order to obtain a fully automated approach, as the subsequent thresholding alone did not produce the desired results.

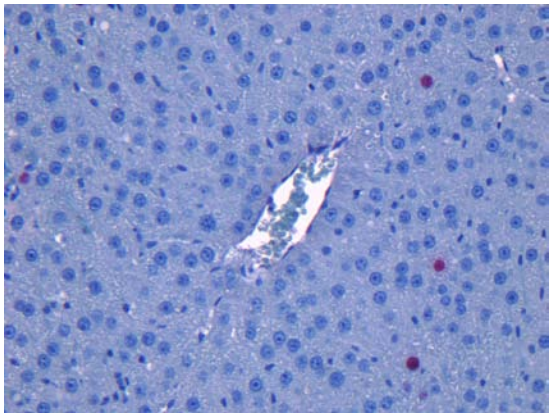

Figure 4: An image with a vein structure. Such images have not been considered in our tests so far.

Acknowledgment

We thank Ms. Ines Krimphoff from University Hospital Essen for image capturing and manual determination of total hepatocyte number.
This work was partially supported by a grant of the German Research Foundation, KFO 117.

References

[AMG98] AURICH V., MÜHLHAUS E., GRUNDMANN S.: Kantenerhaltende Glättung von Volumendaten bei sehr geringem Signal-Rausch-Verhältnis. In *Bildverarbeitung für die Medizin* (1998).

[BL98] BAMFORD P., LOVELL B.: Unsupervised cell nucleus segmentation with active contours. *Signal Processing 71* (1998), 203–213.

[DD02] DURAND F., DORSEY J.: Fast bilateral filtering for the display of high-dynamic-range images. In *ACM Transactions of Graphics (Proceedings of the ACM SIGGRAPH Conference)* (2002), vol. 21, pp. 257–266.

[DMC*08] DIRSCH O., MADRAHIMOV N., CHAUDRI N., DENG M., MADRAHIMOVA F., SCHENK A., DAHMEN U.: Recovery of liver perfusion after focal outflow obstruction and liver resection. *Transplantation 85*, 5 (2008), 748–756.

[DPC08] DATAR M., PADFIELD D., CLINE H.: Color and texture based segmentation of molecular pathology images using hsoms. In *IEEE International Symposium on Biomedical Imaging: From Nano to Macro* (2008), pp. 292–295.

[Hou59] HOUGH P.: Machine analysis of bubble chamber pictures. In *Proc. Int. Conf. High Energy Accelerators and Instrumentation* (1959).

[KBRB07] KORDE V., BARTELS H., RANGER-MOORE J., BARTON J.: Automatic segmentation of cell nuclei in bladder and skin tissue for karyometric analysis. In *Biophotonics 2007: Optics in Life Science. Edited by Popp, Jürgen; von Bally, Gert. Proceedings of the SPIE.* (2007), vol. 6633, p. 66330V.

[Lec89] LECLERC Y.: Constructing simple stable descriptions for image partitioning. *International Journal of Computer Vision 3* (1989), 73–102.

[LSP03] LATSON L., SEBEK B., POWELL K.: Automated cell nuclear segmentation in color images of hematoxylin and eosin-stained breast biopsy. *Analytical and Quantitative Cytology and Histology 25*, 6 (2003), 321–331.

[NA02] NIXON M., A.AGUADO: *Feature extraction and image processing*. Newnes, 2002.

[NDA*08] NAIK S., DOYLE S., AGNER S., MADABHUSHI A., FELDMAN M., TOMASZEWSKI J.: Automated gland and nuclei segmentation for grading of prostate and breast cancer histopathology. In *IEEE International Symposium on Biomedical Imaging: From Nano to Macro* (2008), pp. 284–287.

[Ots79] OTSU N.: A threshold selection method from gray-level histograms. *IEEE Transactions on Systems, Man, and Cybernetics 9*, 1 (1979), 62–66.

[PD06] PARIS S., DURAND F.: A fast approximation of the bilateral filter using a signal processing approach. In *European Conference on Computer Vision* (2006).

[PGH*06] PETUSHI S., GARCIA F., HABER M., KTSINIS C., TOZEREN A.: Large-scale computations on histology images reveal grade-differentiating parameters for breast cancer. *BMC Medical Imaging 6* (2006).

[PM90] PERONA P., MALIK J.: Scale-space and edge detection using anisotropic diffusion. *IEEE Trans. Pattern Anal. Mach. Intell. 12* (1990), 629–639.

[Ris87] RISSANEN J.: Minimum description length principle. *Encyclopedia of Statistical Sciences* (1987).

[RNS*06] RADTKE A., NADALIN S., SOTIROPOULOS G., MOLMENTI E., SCHROEDER T., VALENTIN-GAMAZO C., LANG H., BOCKHORN M., PEITGEN H. O., BROELSCH C. E., MALAGO M.: Computer-assisted operative planning in adult living donor liver transplantation: A new way to resolve the dilemma of the middle hepatic vein. *World J Surg. 31*, 1 (2006), 175–185.

[TM98] TOMASI C., MANDUCHI R.: Bilateral filtering for gray and color images. In *Proceedings of the International Conference on Computer Vision* (1998).

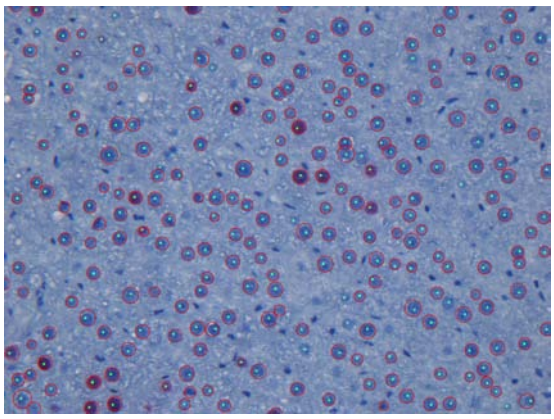

(a) Result of manual thresholding without any smoothing filter applied.

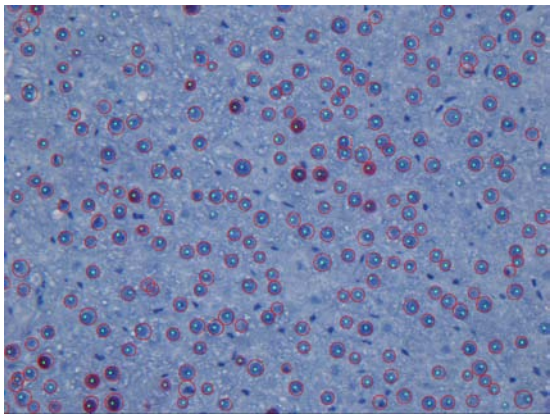

(b) Gaussian smoothing is used as a preprocessing step. As this smoothing does preserve the boundaries, some False Positives arise.

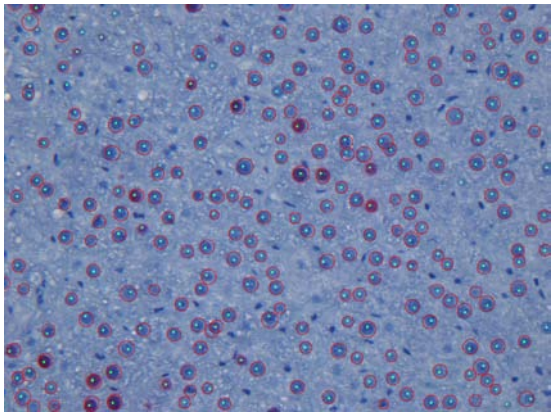

(c) Nonlinear Gaussian smoothing is used as a preprocessing step. Reasonable results are obtained, both in sensitivity and specificity.

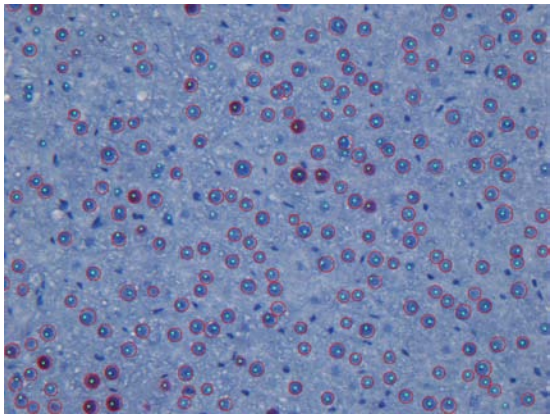

(d) Median filtering is used as a preprocessing step. The number of False negatives is relatively high.

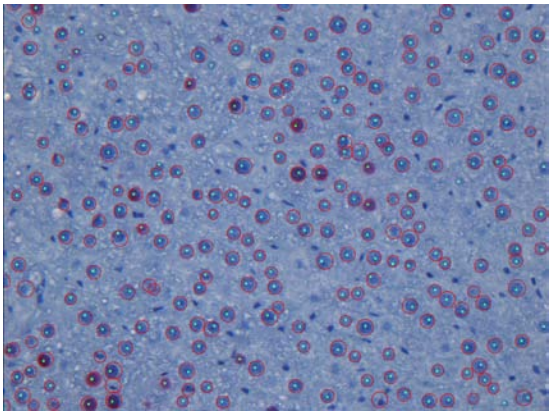

(e) Anisotropic diffusion is used as a preprocessing step. Reasonable results are obtained, both in sensitivity and specificity.

Figure 5: Overlaying the output of the Hough transform (red circles) with the manually specified output (green dots) for image AEE-16-1.